The GOES-R Advanced Baseline Imager and the Continuation of Current Sounder Products

TIMOTHY J. SCHMIT,* JUN LI,+ JAMES J. GURKA,# MITCHELL D. GOLDBERG,@ KEVIN J. SCHRAB,& JINLONG LI,+ AND WAYNE F. FELTZ+

*NOAA/NESDIS Satellite Applications and Research, Advanced Satellite Products Branch, Madison, Wisconsin
+Cooperative Institute for Meteorological Satellite Studies, University of Wisconsin—Madison, Madison, Wisconsin
#NOAA/NESDIS GOES-R Program Office, Greenbelt, Maryland
@NOAA/NESDIS Satellite Applications and Research, Camp Springs, Maryland
&NOAA/NWS Office of Science and Technology, Silver Spring, Maryland

(Manuscript received 23 August 2007, in final form 12 March 2008)

ABSTRACT

The first of the next-generation series of Geostationary Operational Environmental Satellites (GOES-R) is scheduled for launch in the 2015 time frame. One of the primary instruments on GOES-R, the Advanced Baseline Imager (ABI), will offer more spectral bands, higher spatial resolution, and faster imaging than does the current GOES Imager. Measurements from the ABI will be used for a wide range of qualitative and quantitative weather, land, ocean, cryosphere, environmental, and climate applications. However, the first and, likely, the second of the new series of GOES will not carry an infrared sounder dedicated to acquiring high-vertical-resolution atmospheric temperature and humidity profiles that are key to mesoscale and regional severe-weather forecasting. The ABI will provide some continuity of the current sounder products to bridge the gap until the advent of the GOES advanced infrared sounder. Both theoretical analysis and retrieval simulations show that data from the ABI can be combined with temperature and moisture information from forecast models to produce derived products that will be adequate substitutes for the legacy products from the current GOES sounders. Products generated from the Spinning Enhanced Visible and Infrared Imager (SEVIRI) measurements also demonstrate the utility of those legacy products for nowcasting applications. However, because of very coarse vertical resolution and limited accuracy in the legacy sounding products, placing a hyperspectral-resolution infrared sounder with high temporal resolution on future GOES is an essential step toward realizing substantial improvements in mesoscale and severe-weather forecasting required by the user communities.

1. Introduction

As we prepare for the next generation of geostationary satellites, it is important to ensure the continuity and quality of products that users depend on from the current satellite series. The Geostationary Operational Environmental Satellite (GOES) sounders (Menzel and Purdom 1994) have provided quality hourly radiances and derived products over the continental United States and adjacent oceans for over a decade (Menzel et al. 1998; Daniels et al. 2001; Hillger et al. 2003). The derived products include clear-sky radiances, temperature and moisture profiles, total precipitable water vapor (TPW) and layer precipitable water, atmospheric stability indices such as convective available potential energy and lifted index (LI), cloud-top properties (Schreiner et al. 2001), clear-sky water vapor winds through radiance tracking (Velden et al. 1998), and total column ozone (Li et al. 2007; Li et al. 2001). These products are used for a number of numerical weather prediction (NWP) and forecasting applications (Menzel and Purdom 1994; Bayler et al. 2000; Dostalek and Schmit 2001; Schmit et al. 2002). The *GOES-13*/O/P sounders will continue this mission of nowcasting (short-term forecasts) and NWP support. *GOES-13* is the current on-orbit spare, and GOES-O and GOES-P have not yet been launched.

The next-generation geostationary satellite series will enable many improvements and new capabilities for imager-based products. Given that GOES-R will not

Corresponding author address: Timothy J. Schmit, 1225 West Dayton St., Madison, WI 53706.
E-mail: tim.j.schmit@noaa.gov

DOI: 10.1175/2008JAMC1858.1

host a sounding instrument, the question becomes whether the products based on the Advanced Baseline Imager (ABI) will provide an adequate substitute for legacy sounder-based products. The ABI (Schmit et al. 2005) on the next-generation GOES-R will certainly improve upon the current GOES imager with more spectral bands, faster imaging, higher spatial resolution, better navigation, and more accurate calibration. The ABI expands from five spectral bands on the current GOES imagers to a total of 16 spectral bands in the visible (VIS), near-infrared (NIR), and infrared (IR) spectral regions. The coverage rate for full disk scans will increase to at least every 15 min, and the continental U.S. region will be scanned every 5 min. ABI spatial resolution will be 2 km at the subpoint for 10 IR spectral bands, 1 km for select NIR bands, and 0.5 km for the 0.64-μm VIS band (Schmit et al. 2005). However, the ABI was designed assuming a companion high-spectral-resolution IR sounder, originally called the Advanced Baseline Sounder (ABS), and more recently the Hyperspectral Environmental Suite (HES). Consequently, the ABI only has one carbon dioxide (CO_2)-sensitive spectral band. It was envisioned that information from the ABI would improve select products from the HES, such as an improved subpixel characterization through the higher-spatial-resolution information of the ABI (Li et al. 2004a). Also, it was envisioned that information from the HES would improve ABI-based products, including cloud height (through the many spectral bands on the HES) and surface temperature through a better surface emissivity estimate.

The current GOES sounders have 18 infrared spectral bands to profile the atmosphere, and the current GOES imagers have only 4 infrared spectral bands, most of which give surface and cloud information. With the advent of advanced imagers, like the ABI, "legacy sounding–type" products are possible. However, the broadband imager spectral coverage cannot match the performance of high-spectral-resolution advanced sounders. The imagers have spectral resolution (SR) on the order of 50–200 cm^{-1} for a single band, whereas advanced sounders have spectral coverage on the order of 0.5 cm^{-1} for a single channel. The finer resolutions enable measurements of important spectral changes that result from vertical structures and other phenomena. Nevertheless, with the current four-IR-spectral-band imager, certain products like TPW, LI, and skin temperature have been produced (Hayden et al. 1996), evolving from experience with GOES Visible and Infrared Spin-Scan Radiometer (VISSR) and VISSR Atmospheric Sounder (VAS) data (Smith et al. 1985).

Without a high-spectral-resolution sounder on GOES-R/S, legacy sounder products that are used by the National Weather Service and others must still be continued. In this paper, we will show that adequate substitute products can be generated from ABI data, in conjunction with information from short-term numerical model forecasts. The "continuity" products produced from today's low-spectral-resolution sounder include TPW, LI, skin temperature, cloud-top information, and satellite-derived winds.

To understand how the ABI may produce adequate continuity products, the attributes (temporal, spatial, spectral, and radiometric) of each instrument need to be understood. The ABI has improved temporal (Fig. 1) and spatial (Fig. 2) resolutions relative to those of the *GOES-13*/O/P sounders. To showcase the improved spatial resolution of the ABI, *Terra* Moderate-Resolution Imaging Spectroradiometer (MODIS; 1915–1925 UTC 20 July 2002) data were used for Fig. 2. The improved ABI spatial resolution allows for a better clear-sky determination. Both the ABI and the current GOES sounder offer multispectral measurements (Fig. 3). The width of the boxes represents the 50% points in the spectral response functions (SRF). The corresponding weighting functions for the ABI and current sounder are shown in Fig. 4; the current sounder has more CO_2 and shortwave bands than does the ABI that enable better profile retrieval accuracies. The weighting functions are defined as the change of the total transmittance with pressure and reflect the radiance sensitivity to the atmospheric state at the given pressure layer.

It will be shown that the ABI, with numerical model forecast information used as the background, will be slightly inferior to the *GOES-13*/O/P sounder performance, yet both are substantially less capable than a high-spectral-resolution sounder with respect to information content and retrieval accuracy. Current GOES sounder information clear-sky radiances in bands 1–15 (14.7–4.4 μm) are assimilated in the NWP models and will be replaced by ABI bands 7–16 (3.9–13.3 μm), which include only one CO_2 sounding band. Information from the Cross-Track Infrared Sounder (CrIS) and other polar-orbiting high-spectral-resolution IR sounders in conjunction with the finer-spatial-resolution ABI data may provide a useful substitute for current sounder temperature information for radiance uses within NWP. Research has shown the benefits of combining high-spectral-resolution IR sounder measurements with high-spatial-resolution imager data (Li et al. 2004b, 2005a). For NWP assimilation of GOES sounder measurements, moisture is the key. For information content, both the ABI and current sounder have three broad "water vapor" (H_2O absorption) bands and long-

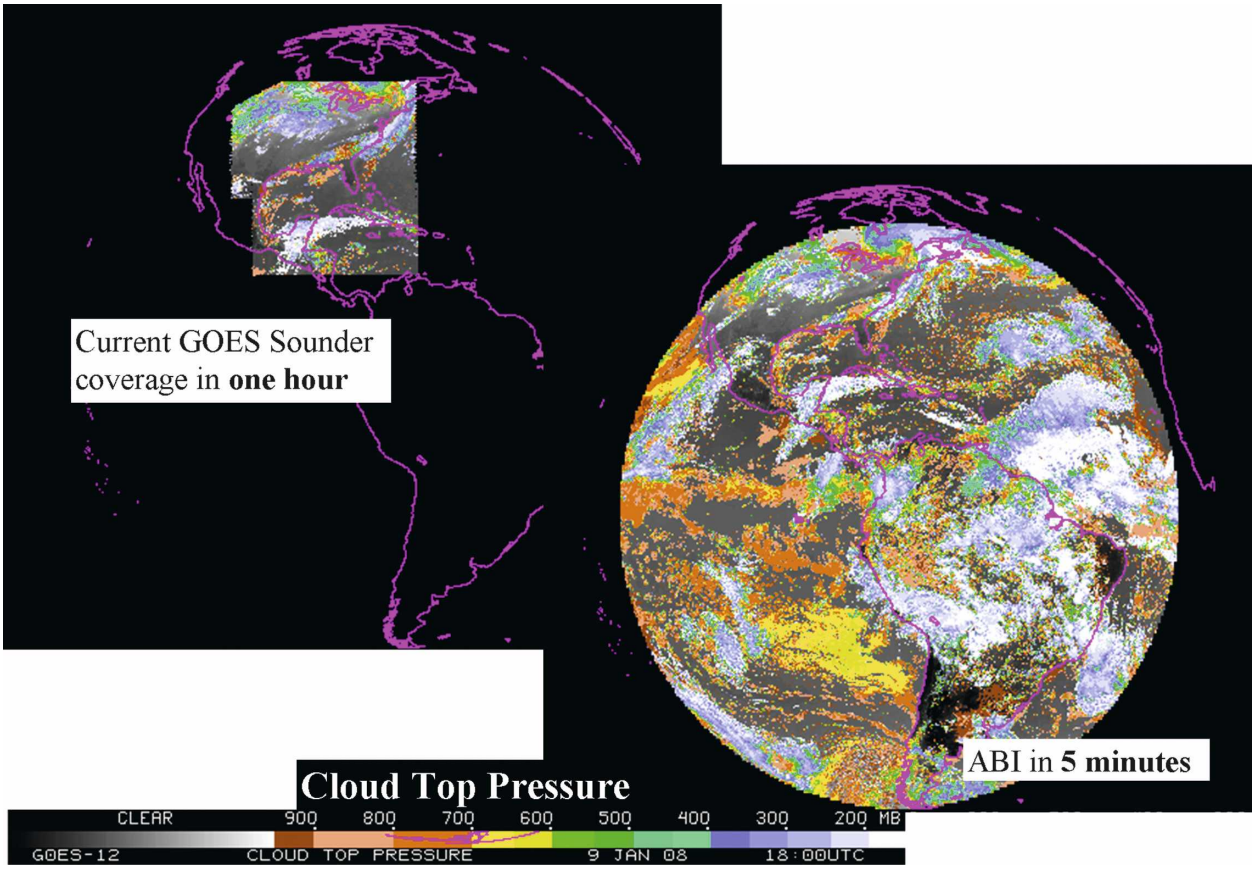

FIG. 1. CTP from the *GOES-12* sounder and *GOES-12* imager. Note the much improved coverage with ABI over the current GOES sounder. The nearly full disk image is derived from *GOES-12* imager data.

wave window bands. However, an HES-type sounder (Wang et al. 2007) with faster scanning and high spectral resolution remains essential for regional NWP, surface emissivity, better nowcasting products, moisture profiles, moisture flux, better cloud heights, and many additional environmental applications.

Section 2 discusses legacy operational products and their potential accuracies achievable with ABI data.

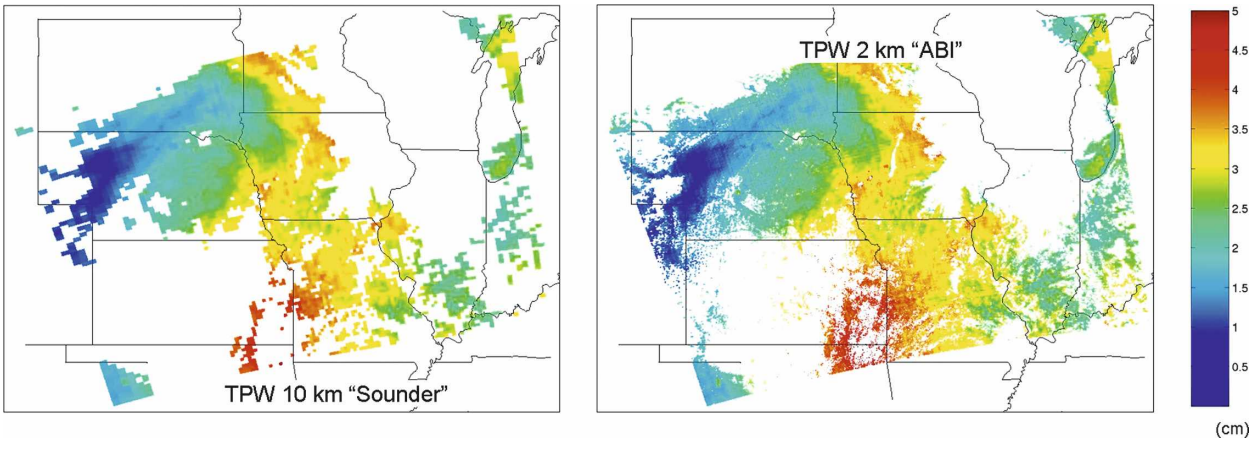

FIG. 2. Simulated (from MODIS) TPW retrievals with (left) 10- and (right) 2-km spatial resolution; 1-km-spatial-resolution MODIS data are used in the simulation. The figure shows improved spatial resolution with ABI over the current sounder. The bluer colors denote drier air, and the redder regions denote higher moisture amounts.

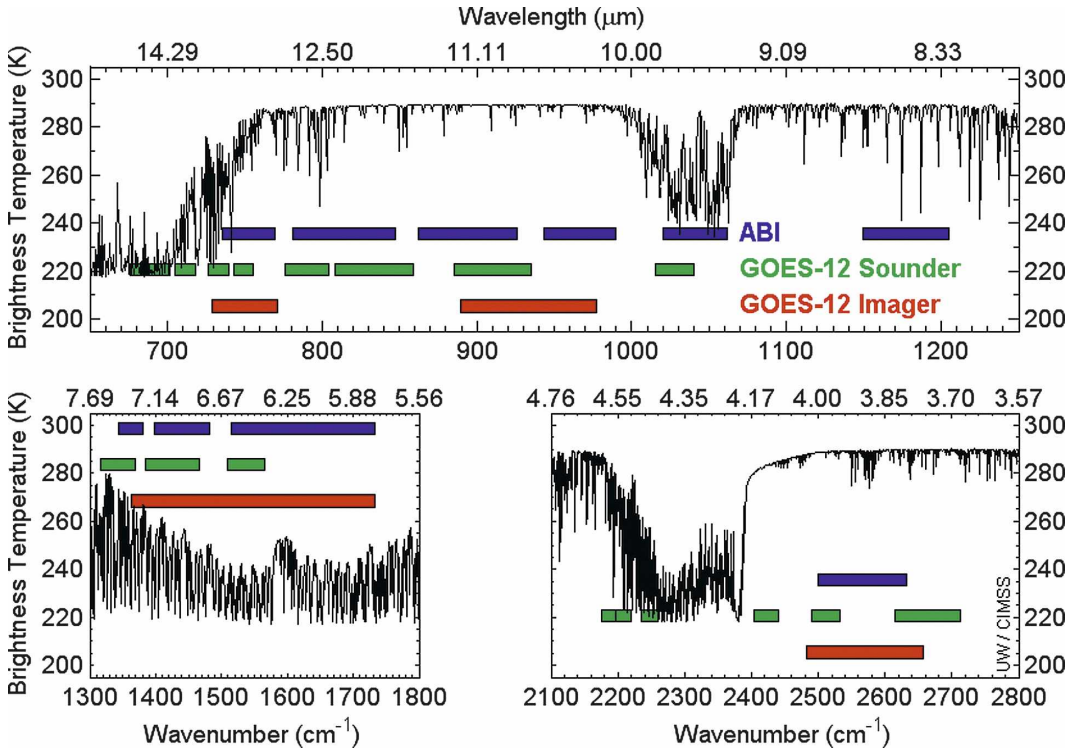

FIG. 3. ABI (blue) and current GOES sounder (green) spectral coverage over a high-spectral-resolution brightness temperature spectrum.

Section 3 introduces several current sounder experimental products that ABI will be able to produce. Section 4 discusses the benefits of using information that has high spatial resolution and high temporal resolution. A product demonstration using the Spinning Enhanced Visible and Infrared Imager (SEVIRI) measurements from the European Meteosat Second Generation (MSG) is given in section 5. Conclusions are presented in section 6.

2. Operational products

Moisture information (three layers of precipitable water) and cloud heights from the current GOES sounders have provided a positive impact on NWP, and nowcasting at the forecast offices has benefited most from atmospheric stability trends. A number of papers document various applications and NWP impacts of hourly GOES sounding data [for examples of applications see Menzel et al. (1998) and for a comparison of geosynchronous-orbit/low-Earth-orbit/radiosonde NWP impact see Zapotocny et al. (2002)].

The ABI will be required to continue the current GOES sounder operational services. Because it has many of the necessary spectral bands and improves upon the spatial coverage of the current sounders, the ABI will be able to provide adequately the required continuity sounder products, including radiances, TPW, LI, skin temperature, clouds, and moisture winds (Table 1). Current GOES sounder clear-sky radiances are used in the assimilation for both regional and global models. The ABI will have instrument noise values that are comparable to those of the current sounder, when the differing detector sizes are taken into account. Plus, the ABI, with its finer spatial resolution, will allow improved clear-sky "hole hunting" relative to the current sounder. Hence, ABI radiance data should be at least as useful to NWP as data from the current GOES sounder to improve the moisture information in the analysis. In fact, because of the much-improved spatial coverage, the ABI data may be preferred for global model applications. Some of these products, such as TPW, are being produced from broadband MODIS data (Seemann et al. 2003), implying that a similar product could be generated from the broadband ABI data. Consequently, it is thought that the current GOES (broad spectral band) sounders (Schmit et al. 2006; Hillger and Schmit 2007) do not offer enough extra capability over the ABI information to warrant their inclusion in the GOES-R series. Because the cov-

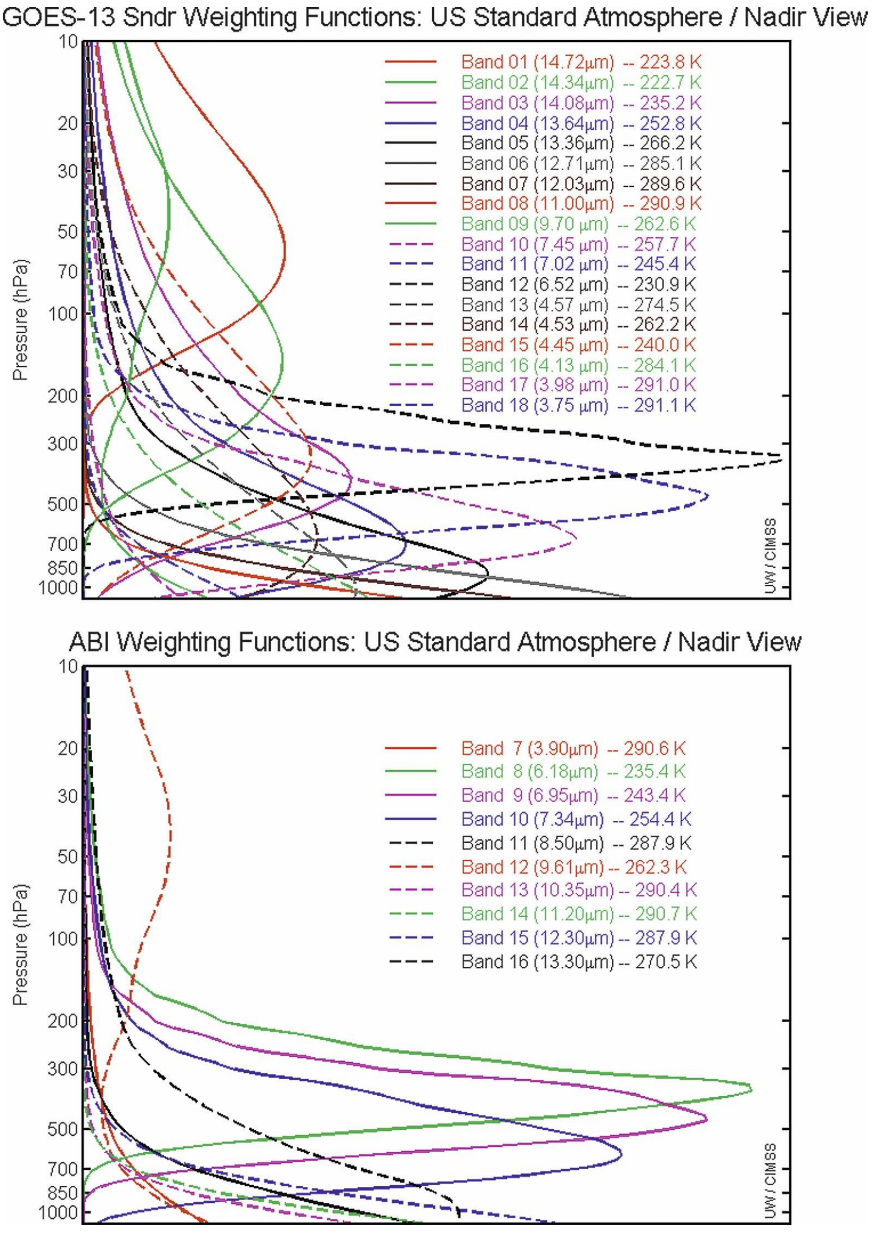

FIG. 4. Weighting functions of the (top) GOES-N sounder and (bottom) ABI. The GOES-N sounder has five CO_2 bands, whereas the ABI only has one. The sounder also has more shortwave bands.

erage rate of the ABI is more than 20 times as fast as that of the current GOES sounder, the ABI offers much greater spatial coverage and much reduced time latency between the satellite observations and associated derived products. Hence, the ABI time-sequence loops of TPW and LI can be produced at finer temporal resolutions than the hourly images from the current sounder. The spatial resolution represented by the footprint size is more than 20 times as fine (changing from approximately 10 km to 2 km in both directions) than that from the current GOES sounders, although some products may need spatial averaging to improve the ABI signal-to-noise ratio. Another possible option to improve the signal-to-noise ratio is to temporally average the radiances (Plokhenko et al. 2003).

a. Theoretical analysis

To compare the profile information between ABI and the current GOES sounder, an error-analysis

TABLE 1. Operational products from the current GOES sounder and how the ABI measurements, along with ancillary data, could help to produce legacy products. Overall, for continuity only, each product is adequately represented.

Product	Temporal/latency	Spatial	Accuracy	Comments
Radiances	ABI is ~20 times faster	Comparable (when averaged)	Comparable for moisture information	Only one CO_2 band on ABI (five bands on sounder)
TPW	ABI is ~20 times faster	Comparable (when averaged)	Sounder is more precise	ABI product quality is helped with model information
LI	ABI is ~20 times faster	Comparable (when averaged)	Sounder is more precise	ABI product quality is helped with model information
Skin temperature	ABI is ~20 times faster	Comparable (when averaged)	Comparable	ABI has extra window band
Profiles	ABI is ~20 times faster	Comparable (when averaged)	Sounder is more precise	Worse upper-level temperature and lower-level moisture
Clouds	ABI is ~20 times faster	ABI is finer	Sounder is more precise for cloud height	Current sounder with more CO_2 bands gives a better height
Moisture winds	ABI is ~20 times faster	ABI is finer	Comparable	—

method is used to demonstrate the profile information theoretically achievable from ABI versus the current GOES sounders. Although the retrieval of temperature and moisture profiles from IR radiances is an ill-posed problem, it can be resolved by the addition of background data from short-term temperature and moisture forecasts. Variational retrievals provide an optimal method of combining observations with a background from a short-term forecast NWP model, accounting for the assumed error characteristics of both the observation and background. The variational retrieval is performed by adjusting the atmospheric profile state $\mathbf{X}$ from the background $\mathbf{X}^b$ to minimize a cost function (Rodgers 1990) of

$$J(\mathbf{X}) = [\mathbf{Y}^m - F(\mathbf{X})]^{\mathrm{T}}\mathbf{E}^{-1}[\mathbf{Y}^m - F(\mathbf{X})] + (\mathbf{X} - \mathbf{X}^b)^{\mathrm{T}}\mathbf{B}^{-1}(\mathbf{X} - \mathbf{X}^b). \quad (1)$$

In Eq. (1), $\mathbf{B}$ and $\mathbf{E}$ are the error covariance matrices of the background vector $\mathbf{X}^b$ and the observation (radiances) vector $\mathbf{Y}^m$, respectively, $F(\mathbf{X})$ is the forward radiative transfer model (RTM) operator, and superscripts T and -1 are the matrix transpose and inverse, respectively.

By using Newtonian iteration [solving equation $J'(\mathbf{X}) = 0$],

$$\mathbf{X}_{n+1} = \mathbf{X}_n - [J''(\mathbf{X}_n)]^{-1}J'(\mathbf{X}_n), \quad (2)$$

the following quasi-nonlinear iterative form is obtained:

$$\delta\mathbf{X}_{n+1} = (F_n'^{\mathrm{T}}\mathbf{E}^{-1}F_n' + \mathbf{B}^{-1})^{-1}F_n'^{\mathrm{T}}\mathbf{E}^{-1}(\delta\mathbf{Y}_n + F_n'\delta\mathbf{X}_n), \quad (3)$$

where $\delta\mathbf{X}_n = \mathbf{X}_n - \mathbf{X}^b$, $\delta\mathbf{Y}_n = \mathbf{Y}^m - F(\mathbf{X}_n)$, F' is the tangent linear operative (Jacobian) of forward model F, and n is the iteration index.

A fast RTM called Pressure-Layer Fast Algorithm for Atmospheric Transmittances (PFAAST; Hannon et al. 1996) was used in this study for the ABI and the *GOES-13*/O/P sounders; this model has 101 pressure levels, ranging from 0.05 to 1100 hPa. The fast transmittance model parameterization was developed using line-by-line RTM calculations and the high-resolution transmission molecular absorption spectroscopic database HITRAN 2000. The calculations take into account the satellite zenith angle, absorption by well-mixed gases (including nitrogen, oxygen, and CO_2), water vapor (including the water vapor continuum), and ozone. The ABI SRF is assumed to be a combination of "Gaussian" and "boxcar" functions in that the wings fall off similar to a Gaussian distribution but the top of the SRF is spectrally flat, similar to ideal boxcar functions (Schmit et al. 2005).

An estimate of the uncertainty of the retrieved profile can be derived by assuming that the errors are normally distributed about the solution and that the problem is only moderately nonlinear. An RTM error of 0.2 K was assumed for all wavelengths. In such a case, the theoretically possible error covariance matrix of the analysis $\mathbf{A}$ is given by

$$\mathbf{A} = (F_f'^{\mathrm{T}}\mathbf{E}^{-1}F_f' + \mathbf{B}^{-1})^{-1}, \quad (4)$$

where F_f' is the weighting function evaluation at the solution (or final iteration), calculated analytically (Li 1994). Although $\mathbf{A}$ depends on the reference profile, it has been evaluated for ABI, the current GOES sounder, and HES (final formulation) in a U.S. standard atmosphere in Fig. 5; only the square roots of diagonal values are used. For the simulations, the specified Performance and Operational Requirements Document noise values were used for HES (Wang et al. 2007). The coverage and SR used was 675–1200 cm^{-1}

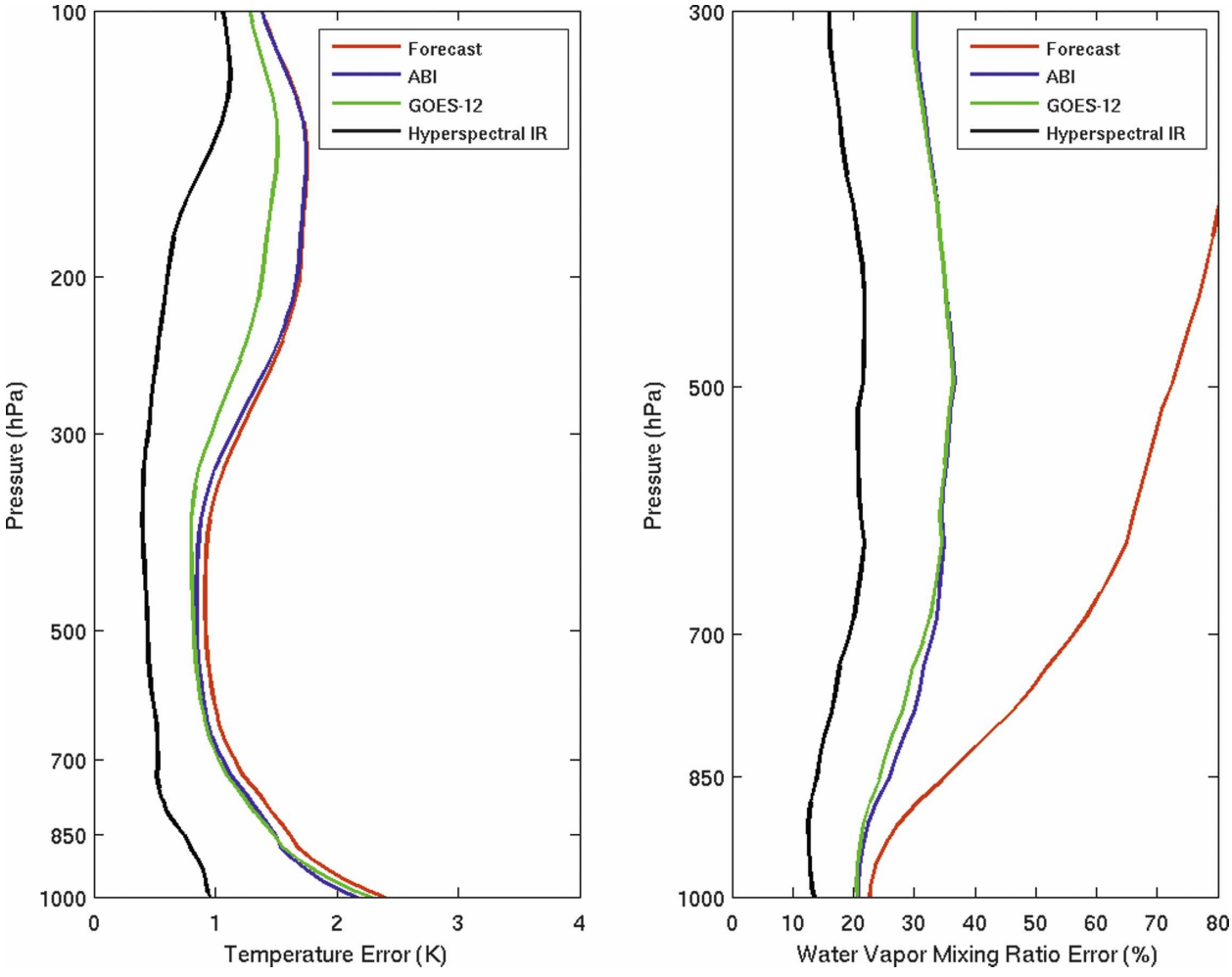

FIG. 5. (left) Temperature and (right) water vapor mixing ratio background error covariance matrix from forecast model (**B**) and analysis error covariance matrices (**A**) with ABI, *GOES-12* sounder, and HES final formulation. Each analysis is based on the same background derived from the forecast information.

with 0.625 cm^{-1} SR, 1689–2150 cm^{-1} with 1.250 cm^{-1} SR, and 2150–2400 cm^{-1} with 2.50 cm^{-1} SR.

The background error covariance matrix is derived from a matchup dataset containing spatially and temporally collocated radiosondes, *GOES-12* sounder radiances, and forecast (the National Centers for Environmental Prediction Global Model) information over the continental United States (CONUS). The radiosondes used in the analysis are independent of the training datasets. The left panel of Fig. 5 shows that both the ABI and the current sounder provide slightly improved temperature information to the forecast, yet the current GOES sounder provides more temperature information beyond the forecast, especially higher in the atmosphere. Using the current GOES algorithm for the temperature retrieval, the upper-level temperature is only changed slightly (Ma et al. 1999). High-spectral-resolution data, on the other hand, provide significant temperature improvement over the forecast. The right panel of Fig. 5 shows that for the water vapor error covariance matrix the ABI error is similar to that of the current GOES sounder. Both have three broad water vapor spectral bands; both instruments improve the forecast information that shows a large water vapor background error. Again, the high-spectral-resolution data provide water vapor information of much higher quality than do either the current GOES sounder or ABI.

b. Retrieval simulation

Matrix **A** presents a theoretical analysis for specific profiles to show the possible error for a given sensor; **A** does not represent the retrieval error, because the nonlinear and inverse errors are not included in **A** (Huang

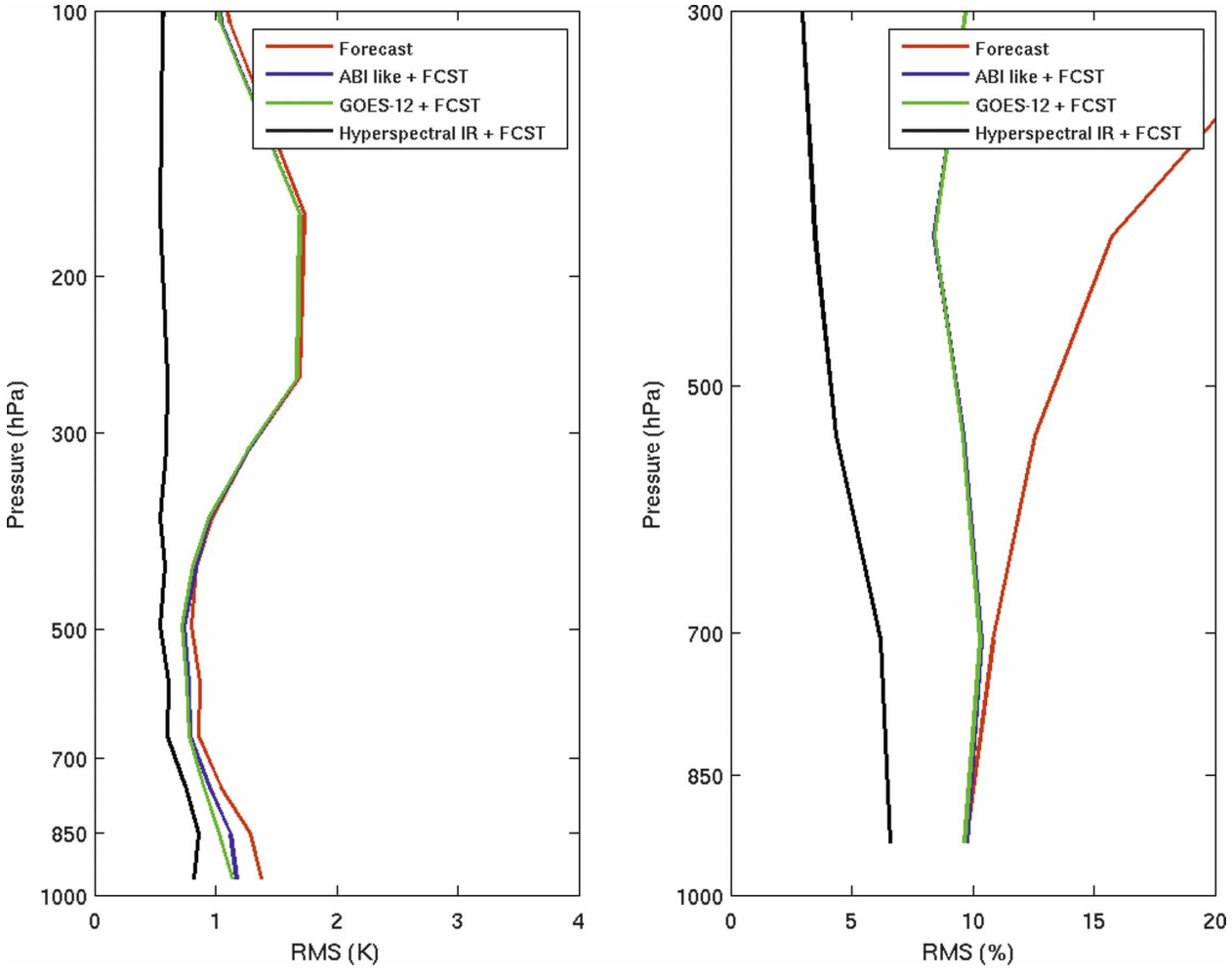

FIG. 6. The (left) 1-km-vertical-layer temperature and (right) 2-km-vertical-layer relative humidity retrieval RMSE with ABI-like retrievals, *GOES-12* sounder, and HES. The forecast information is included in the retrieval.

et al. 1992). To compare further the retrieval performance of ABI, the current GOES sounder, and HES, a retrieval simulation was performed. The simulation used the matchup dataset mentioned above. The *GOES-12* sounder radiance measurements, "ABI radiances" selected from the *GOES-12* sounder radiance measurements, and high-spectral-resolution radiances simulated from the radiosondes through radiative transfer calculations were used to compute temperature and moisture profile retrievals. The instrument noise was randomly added to the HES simulated radiances. The radiosonde profiles were used as truth in the generation of all the statistics. The retrieval method used consists of a statistical technique followed by a physical iterative approach [see Eq.(3) for physical iteration] (Li and Huang 1999; Li et al. 2000). The first guess from the statistical technique was based on a near-global training dataset (obtained online at http://cimss.ssec.wisc.edu/training_data/) that contained realistic IR surface emissivity and skin temperature information.

Figure 6 shows the 1-km-vertical-layer temperature retrieval root-mean-square error (RMSE) (left panel) and 2-km-vertical-layer relative humidity (RH) RMSE (right panel). The RMSE is based on the absolute differences between retrieval and truth, and the statistics are based on approximately 300 independent retrievals. The simulation shows a slight temperature improvement of *GOES-12* sounder retrievals over the forecast (approximately 0.1–0.2 K in the troposphere). As expected, the ABI-like data have even less temperature information than do the *GOES-12* sounder data. In terms of RH, the *GOES-12* sounder and ABI-like retrievals provide similar retrieval performance, and both improve on the forecast. Again, HES provides the best temperature and water vapor retrievals, with much better accuracies than the forecast, the ABI-like retrievals,

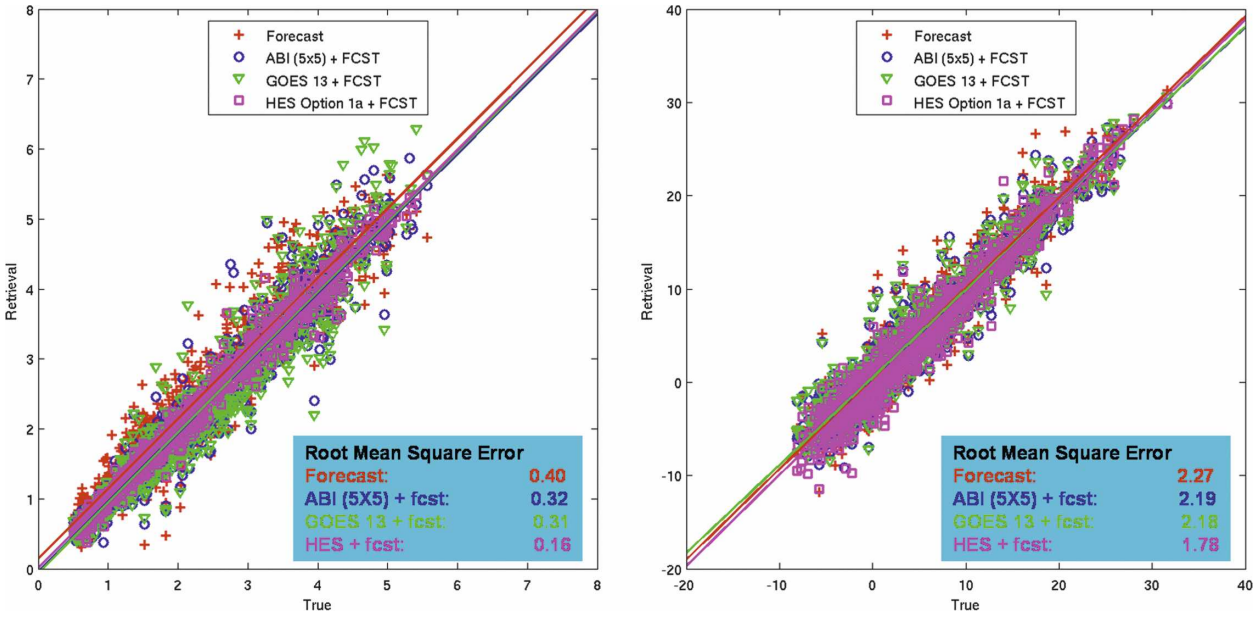

FIG. 7. Simulations of (left) GOES-N TPW and (right) LI performance.

and the current GOES sounder retrievals. This retrieval simulation is consistent with the analysis discussed in section 2a.

The accuracy of several products would be slightly degraded when produced from the ABI rather than from the current GOES sounder. Simulations (using background information) imply that both TPW and LI will be slightly degraded when using ABI, relative to the GOES sounder data. TPW accuracy values show that the ABI plus forecast and the sounder plus forecast improve relative to the forecast alone (Fig. 7). Recall that products such as TPW and LI are valuable to forecasters because they are quickly available for use in nowcasting applications. Simulations show that these retrievals have approximately double the error in terms of the RMS relative to those from a high-spectral-resolution sounder. Spatial (and possibly temporal) averaging of ABI data can help to improve profile accuracy, but the profiles from ABI alone are still degraded relative to those from the current GOES sounder alone. Research with the current GOES sounder has shown the benefits of temporal smoothing (Plokhenko et al. 2003). The ABI and the current GOES sounder profiles are both significantly inferior to those from a high-spectral-resolution sounder. Similar results are found in the simulation of atmospheric stability (e.g., the LI). In the LI calculations, approximately 600 independent profiles were retrieved. The data used for Figs. 5–7 are matchups over the CONUS region.

Derived product images show that cloud-height estimates from the current imager and current sounder are qualitatively comparable (Fig. 1). A quantitative comparison between the imager and sounder cloud-top pressure (CTP) for the day/time shown in Fig. 1 (1800 UTC 9 January 2008) shows a bias of −14 hPa. On average the GOES imager CTP is slightly lower in altitude (higher pressure) than the GOES sounder cloud product. The sample size was 7726. The correlation coefficient was 0.79, although the standard deviation was approximately 245 hPa. Theory indicates that additional CO_2-sensitive bands should improve the height and microphysical property estimate, especially for optically thin/high clouds (Huang et al. 2004; Li et al. 2005b; Weisz et al. 2007). The similarity of imager and sounder cloud-top-height information for a limited number of collocations when compared with an aircraft lidar was documented by Bedka et al. (2007). Information on the validation of clouds from GOES sounder with ground-based lidar data can also be found in Hawkinson et al. (2005).

Some products demonstrate improvement with the ABI over the current GOES sounder. The skin temperature accuracy should be improved, because the ABI has an additional infrared window band (10.35 μm or 966.2 cm^{-1}). GOES sounder moisture winds should also be improved with the ABI because of the improved spatial resolution and improved image quality. In addition, the ABI will allow more flexibility in terms of the time between images than do the fixed hourly images from the current sounder.

TABLE 2. Experimental products from the current GOES sounder and how the ABI measurements, along with ancillary data, could help to produce legacy products. Overall, for continuity only, each product is adequately represented.

Product	Temporal/latency	Spatial	Accuracy	Comments
Total column ozone	ABI is ~20 times faster	Comparable (when averaged)	Sounder is more precise	Sounder is better because of several CO_2 bands
Microburst potential	ABI is ~20 times faster	Comparable (when averaged)	Sounder is more precise	Profiles are used as inputs
Other stability products	ABI is ~20 times faster	Comparable (when averaged)	Sounder is more precise	Profiles are used as inputs
Upper-level SO_2	ABI is ~20 times faster	Comparable (when averaged)	ABI more is precise	ABI has an additional band
Cloud "climatology"	ABI is ~20 times faster	ABI is finer	Sounder is more precise	Current sounder with more CO_2 bands gives a better height

3. Experimental products

Table 2 lists selected current experimental products from the GOES sounders. Some may become operational products well before the advent of the GOES-R series. Again, the ABI has improved temporal and spatial attributes, although the accuracy will be slightly degraded for some products—for example, the total column ozone (TCO) (Jin et al. 2008). Some products will be produced with a finer accuracy using ABI data [e.g., upper-level detection of sulfur dioxide (SO_2) (Schreiner et al. 2004; Schmit et al. 2005): the ABI has two bands (7.34 and 8.5 μm) that are sensitive to the detection of upper-level SO_2 and moisture winds].

4. Spatial and temporal benefits with ABI

The high spatial and temporal resolutions of ABI data can benefit the legacy products. For example, the radiance noise can be reduced by an averaging process within a 5×5 field-of-view (FOV) area. In such a case, products with 10-km spatial resolution can be achieved with better accuracy than single FOV retrievals with 2-km spatial resolution. The radiance noise may also be reduced through temporal averaging. To quantify the beneficial impact on retrievals realized from the improved spatial resolution, approximately 600 independent near-global (i.e., no polar region data) retrievals were derived for various ABI product resolutions. Averaging of 3×3 and 5×5 FOVs was investigated. Figure 8 shows the temperature (left panel) and RH (right panel) retrieval RMSE for different ABI spatial configurations. Retrievals from GOES-N sounder and HES final formation are also included for comparison purposes. Note that the retrievals are based on the sensor information alone; no NWP forecast information is included in the retrievals. In this simulation, the first guess is from regression derived from the radiances. The training set consisted of global radiosondes, within 65° of the equator.

ABI single FOV (SFOV) provides very limited temperature information; averaging the radiances slightly improves the temperature profile information, especially between 400 and 700 hPa. However, even 5×5 ABI radiance averages provide worse retrievals than the current GOES sounder SFOV radiances; despite three water vapor bands to provide some temperature information, the ABI has only one CO_2 absorption band. For relative humidity, the 3×3 retrievals provide a considerable improvement over the SFOV retrievals. The 5×5 retrievals provide better moisture information than the SFOV or 3×3 retrievals. It is interesting to note that 5×5 FOV ABI retrievals are slightly worse than the current GOES sounder SFOV for moisture even though both the ABI and the current GOES sounder have three water vapor absorption spectral bands. This result is due to the fact that the water vapor retrievals also rely on temperature information, because water vapor bands contain both atmospheric emission and absorption. The ABI has fewer CO_2 bands than the GOES sounder. As a consequence, when the ABI and sounder are used alone, the moisture retrievals are worse. With short-term forecast profile information included as a background, ABI and the current GOES sounder provide comparable moisture retrievals.

5. Demonstration with SEVIRI and Atmospheric Emitted Radiance Interferometer (AERI)

The SEVIRI on the first MSG satellite (MSG-1), now called *Meteosat-8*, provides temperature and water vapor information similar to ABI but with slightly lower spatial resolution (resampled to 3 km nominally). The SEVIRI instrument has a similar band configuration to that specified for the ABI, and hence SEVIRI

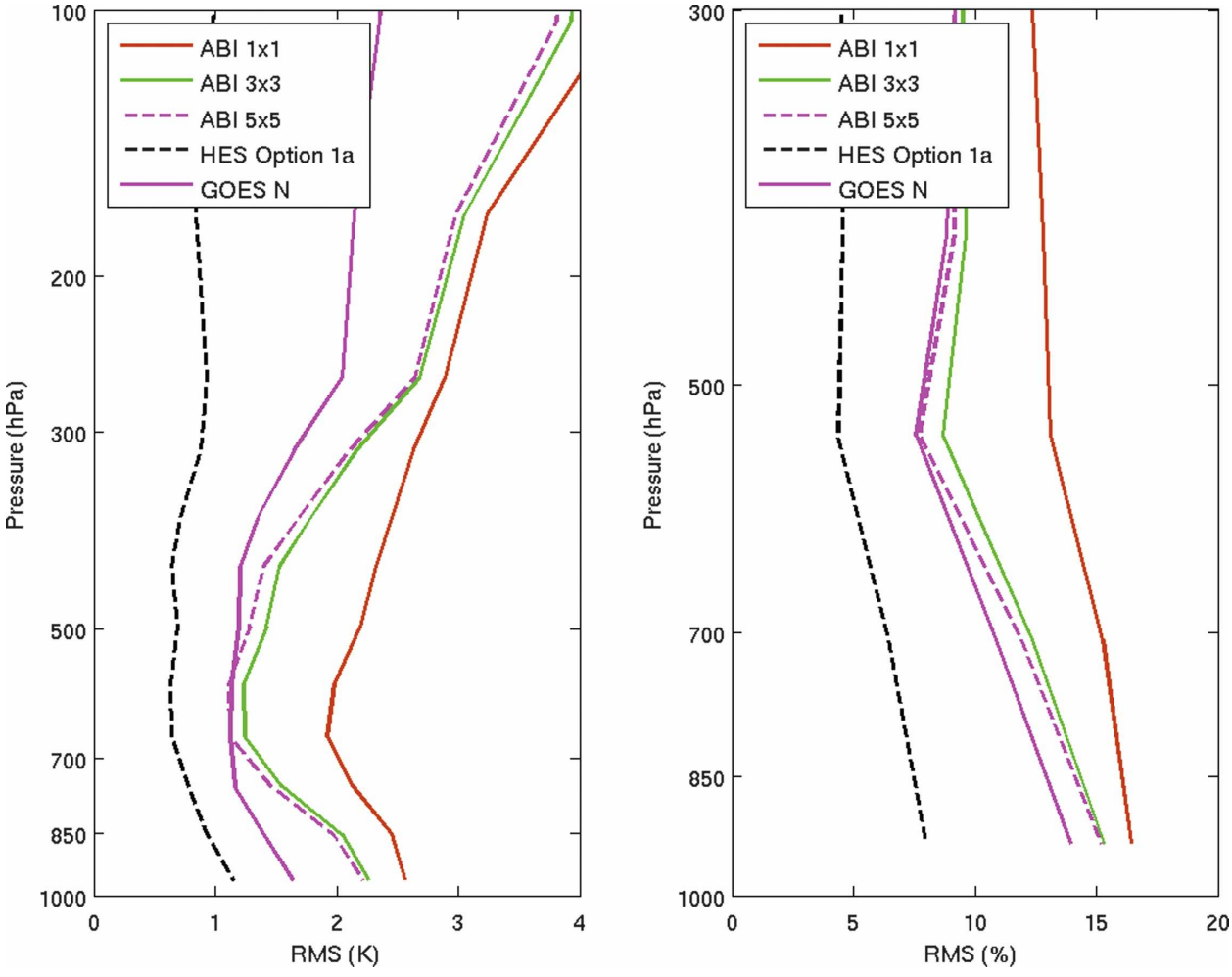

FIG. 8. Simulations of (left) GOES temperature and (right) RH retrieval performance (RMS), using near-global raobs of 600 independent sounding retrievals. The retrieval algorithm is based on regression (first guess) followed by physical (final). No NWP forecast information is included in the retrievals. "GOES-N" denotes the current sounder.

data have been used as a proxy to demonstrate ABI legacy estimates [see Table 3 for SEVIRI instrument characteristics (Aminou et al. 2003)]. However, ABI and SEVIRI differ in some important ways. ABI has two more IR bands than does SEVIRI. ABI is designed for a 5-min full-disk scan at a spatial resolution of 2 km for the IR bands whereas SEVIRI makes a full-disk scan in 15 min with 5-km-sized samples regridded onto a perfect 3-km-resolution projection. The spectral responses of the individual bands and the noise equivalent radiances (NEDR) are different and can lead to different retrieval performance. These differences were evaluated in numerical simulations, such as a study of TCO (Jin et al. 2008). The *GOES-12* sounder radiance noise estimates are from the *GOES-12* National Oceanic and Atmospheric Administration (NOAA) Science Test technical report (Hillger et al. 2003).

We have used SEVIRI measurements and European Centre for Medium-Range Weather Forecasts (ECMWF) forecasts to demonstrate the legacy products possible with ABI-like data. Figure 9 shows the TPW (left panel) and LI (right panel) retrievals from SEVIRI at 1200 UTC 14 February 2006. An ECMWF 6-h forecast was used as the first guess. The unstable atmosphere is clearly depicted by SEVIRI over central Africa, and a convective storm complex formed in this region a few hours later. This example supports the assumption that the ABI time-sequence loops of TPW and LI can be used to support "nowcasting" applications by monitoring changes in time, as does the current sounder. Comparisons between the analysis [at radiosonde observation (raob) locations and times] and retrievals (Fig. 10) from the month of August (2006) show that a combination of SEVIRI and the forecast is ca-

TABLE 3. Band number, central wavelength (μm), and NEDR (mW m^{-2} sr^{-1} cm^{-1}) for ABI, SEVIRI, and the *GOES-12* sounder. The ABI NEDR are specification values. Note that the FOV size of the GOES sounder is much larger than that of the ABI and SEVIRI.

GOES-12 sounder			ABI (specification)			SEVIRI		
Band	NEDR	Wavelength	Band	NEDR	Wavelength	Band	NEDR*	Wavelength
18	0.0009	3.75						
17	0.0022	3.98	1		0.47			
16	0.0024	4.12	2		0.64	1		0.635
15	0.0066	4.45	3		0.87	2		0.81
14	0.0062	4.53	4		1.38			
13	0.0062	4.57	5		1.61	3		1.64
12	0.11	6.5	6		2.25			
11	0.059	7.01	7	0.0038	3.9	4	0.0046	3.92
10	0.099	7.44	8	0.058	6.19	5	0.0098	6.2
9	0.14	9.72	9	0.0827	6.95			
8	0.11	10.96	10	0.0958	7.34	6	0.0226	7.35
7	0.11	11.99	11	0.1304	8.5	7	0.0948	8.7
6	0.14	12.66	12	0.1539	9.61	8	0.0975	9.66
5	0.34	13.34	13	0.1645	10.35			
4	0.39	13.63	14	0.1718	11.2	9	0.1247	10.8
3	0.45	14.03	15	0.1754	12.3	10	0.1923	12
2	0.61	14.38	16	0.5237	13.3	11	0.4178	13.4
1	0.77	14.66						

* These values are calculated from in-flight measurements of noise equivalent difference of temperature (NEDT; Aminou et al. 2003).

pable of providing reasonable nowcasting products such as TPW. These retrievals need the benefit of a short-term forecast and could be further improved with more bands of the current sounder or could be greatly improved with high-spectral-resolution IR measurements. Note that the ECMWF analysis may contain some SEVIRI clear-sky water vapor band information (Szyndel et al. 2005). Further analysis will be conducted to compare SEVIRI retrievals of TPW and Earth Observing System (EOS) data—for example, the operational Advanced Microwave Scanning Radiometer for EOS (AMSR-E) product.

As has been shown with the simulations in Figs. 5–8, the high-spectral-resolution IR data are much improved over the broadband data. To illustrate this point further, an example with ground-based high-spectral-

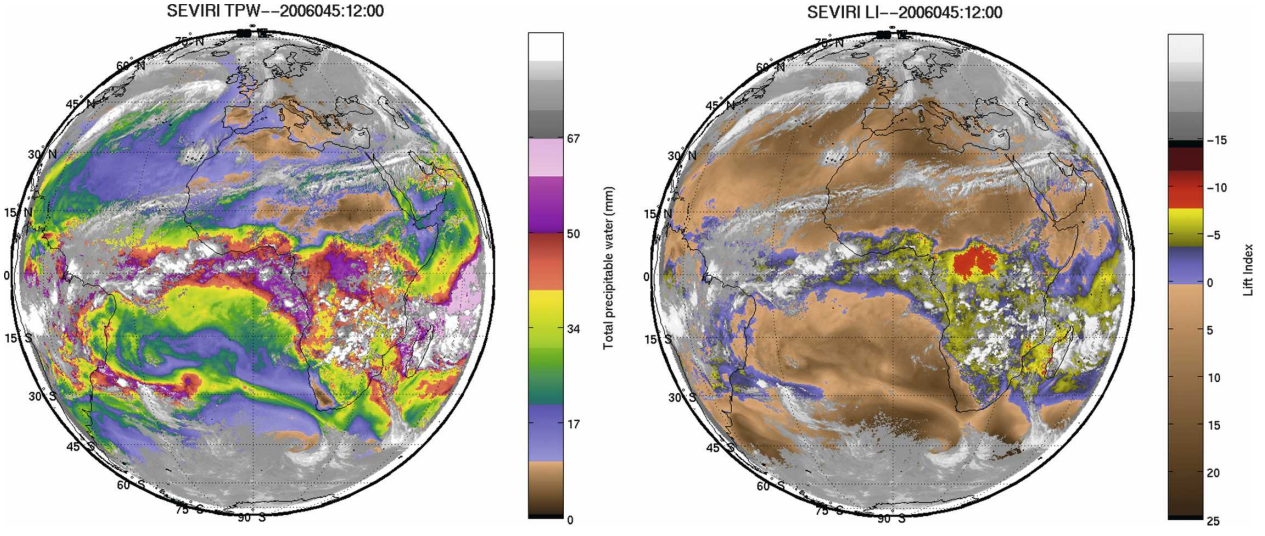

FIG. 9. (left) TPW and (right) LI retrievals derived from SEVIRI at 1200 UTC 14 Feb 2006. The ECMWF 6-h forecast is used as the first guess.

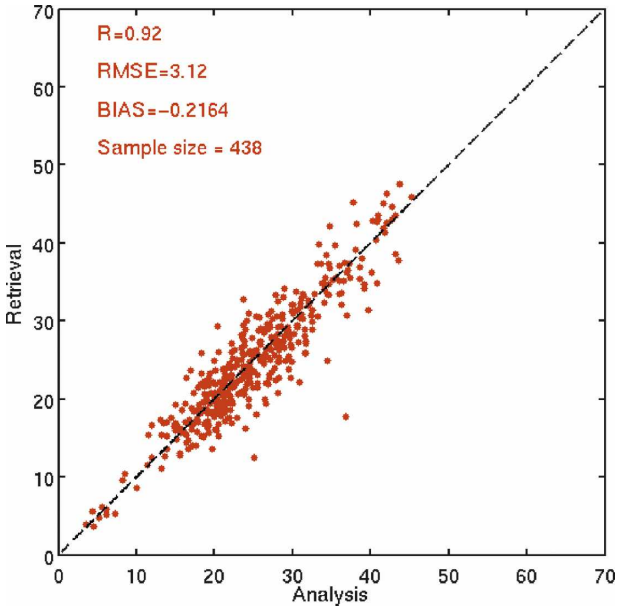

FIG. 10. TPW scatterplot between the ECMWF analysis (at raob locations) and SEVIRI for August 2006.

resolution IR data is provided. The AERI (Knuteson et al. 2004a,b) is an up-looking high-spectral-resolution (finer than 1 cm^{-1}) infrared instrument that monitors planetary boundary layer (PBL) thermodynamic structure at approximately 10-min temporal resolution (Feltz et al. 2003). Up-looking AERI-retrieved water vapor profiles, along with radiosonde data, from the 3 May 1999 Oklahoma/Kansas tornado outbreak (Feltz and Mecikalski 2002) are shown in the top panel of Fig. 11. Representative PBL vertical-resolution functions were applied to the top-panel water vapor field to simulate the hyper-spectral-resolution Geosynchronous Imaging Fourier Transform Spectrometer (GIFTS; Smith et al. 2002) and current GOES sounders. Differences were then taken between the simulated water vapor fields and the "true field" (top panel) to produce the center and lower cross sections within Fig. 11. For this case, the retrievals from the high-spectral-resolution measurements more properly capture the important vertical moisture variations; not only are the errors reduced, but low-level moisture peaks and vertical gradients are captured. These two panels indicate the benefit of high-spectral-resolution IR data over the broadband data for capturing the spatial and temporal variation in the PBL water vapor field important for NWP forecast improvements and short-term atmospheric stability applications.

6. Summary

Theoretical analyses and retrieval simulations both show that data from the ABI can be combined with

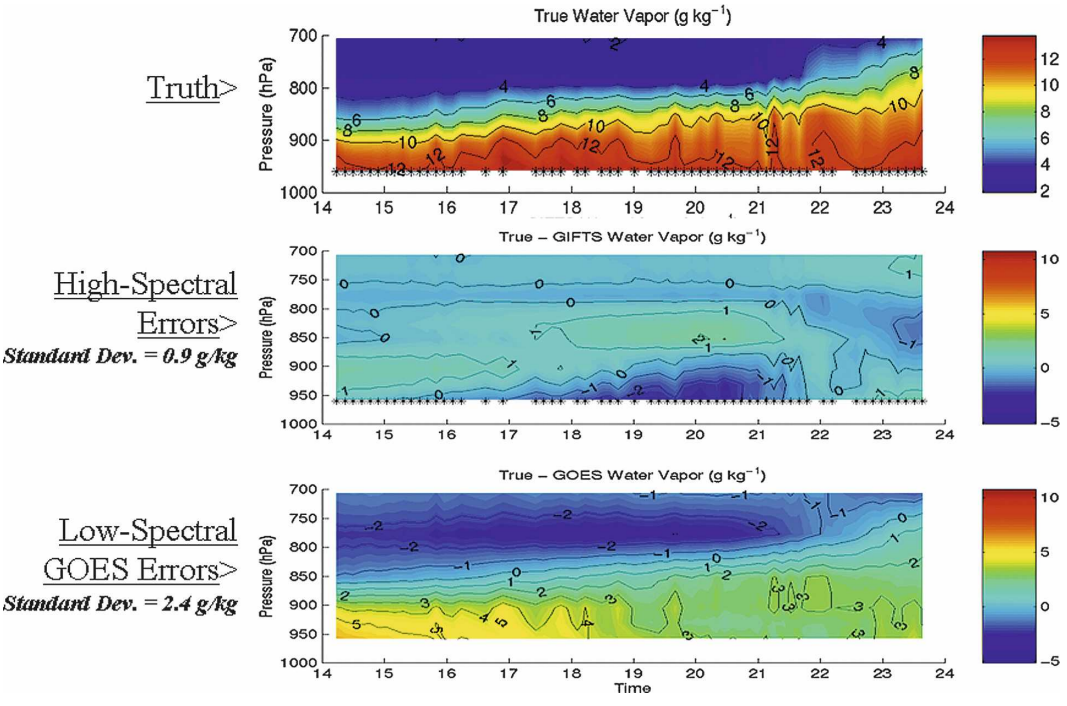

FIG. 11. (top) A time–height cross section of retrieved water vapor (g kg^{-1}) from an up-looking AERI from the 3 May 1999 Oklahoma tornado outbreak. (middle) The difference between the AERI water vapor field from the top panel and simulated hyperspectral water vapor field using representative vertical-resolution functions. (bottom) A similar set of differences except that a GOES vertical-resolution function was used.

temperature and moisture information from a forecast model to produce sounding products that adequately substitute for those produced from the broadband sounders on current GOES satellites. Both the current GOES sounder and ABI can provide additional useful moisture information beyond that available from forecasts alone. The ABI adequately provides continuity of the current GOES sounder operational products; however, it does not meet, as expected, advanced sounding requirements (Figs. 5, 6) needed for future numerical weather prediction (hourly radiances enabling profile retrievals with higher vertical resolution for both temperature and moisture) and severe-weather applications. The ABI was designed to work in conjunction with a high-spectral-resolution sounder. High-spectral-resolution observations are needed for nowcasting, NWP, and many other applications. Without high-spectral-resolution IR geostationary sounding capabilities, forecasters and regional models will not have sufficient information about the finescale three-dimensional structure of atmospheric water vapor and capping inversions. Numerical-model simulation experiments have shown the benefit of high-temporal-resolution data coupled with high-vertical-resolution data for regional models (Aune et al. 2000). Plus, models have shown the benefits of high-spectral-resolution IR AIRS data (Chahine et al. 2006; Le Marshall et al. 2006a,b). A high-spectral-resolution (and hence high vertical resolution) IR sounder with faster scanning is essential to monitor important low-level information. The potential uses (atmospheric profiling, surface characterization, cloud information, chemistry, atmospheric motion vector winds, etc.) of high-spectral-resolution IR data have been documented (Smith et al. 1990, 2002; Hayden and Schmit 1991; Leslie et al. 2002; Knuteson et al. 2004c; Schmidt et al. 2004; Barnet et al. 2003; Revercomb et al. 2004; Velden et al. 2007). Although the ABI will adequately fill the gap with respect to continuity products, the advanced geosynchronous-orbit sounder should be developed as soon as possible.

Acknowledgments. The authors thank the host of CIMSS, NOAA/NESDIS, and other scientists that contributed to the use of the current GOES sounders. We especially thank Dr. W. P. Menzel for his leadership, and J. Daniels is also thanked; A. J. Schreiner supplied Fig. 1, Mathew Gunshor (CIMSS) is thanked for Figs. 3 and 4, and Xin Jin processed the SEVIRI data for Figs. 9 and 10. SEVIRI data were provided by EUMETSAT. This study was partially supported by NOAA GOES-R Grant NA06NES4400002. The views, opinions, and findings contained in this report are those of the authors and should not be construed as an official National Oceanic and Atmospheric Administration or U.S. government position, policy, or decision.

REFERENCES

Aminou, D., and Coauthors, 2003: Meteosat second generation: A comparison of on-ground and on-flight imaging and radiometric performances of SEVIRI on *MSG-1*. *Proc. 2003 EUMETSAT Meteorological Satellite Conf.,* Weimar, Germany, EUMETSAT, 236–243.

Aune, R. M., W. P. Menzel, J. Thom, G. M. Bayler, A. Huang, and P. Antonelli, 2000: Preliminary findings from the geostationary interferometer Observing System Simulation Experiments (OSSE). NOAA Tech. Rep. NESDIS 95, U.S. Dept. of Commerce, Washington, DC, 18 pp.

Barnet, C., S. Datta, and L. Strow, 2003: Trace gas measurements from the Atmospheric Infrared Sounder (AIRS). *Optical Remote Sensing,* OSA Technical Digest, Trends in Optics and Photonics Series, Vol. 85, Optical Society of America, 89–92.

Bayler, G. M., R. M. Aune, and W. H. Raymond, 2000: NWP cloud initialization using GOES sounder data and improved modeling of nonprecipitating clouds. *Mon. Wea. Rev.,* **128,** 3911–3920.

Bedka, S. T., W. F. Feltz, A. J. Schreiner, and R. E. Holz, 2007: Satellite derived cloud top pressure product validation using aircraft based cloud physics lidar data from the AtREC field campaign. *Int. J. Remote Sens.,* **28,** 2221–2239.

Chahine, M. T., and Coauthors, 2006: AIRS: Improving weather forecasting and providing new data on greenhouse gases. *Bull. Amer. Meteor. Soc.,* **87,** 911–926.

Daniels, J. M., T. J. Schmit, and D. W. Hillger, 2001: GOES-11 Science Test: GOES-11 Imager and Sounder radiance and product validations. NOAA Tech. Rep. NESDIS 103, U.S. Department of Commerce, Washington, DC, 49 pp.

Dostalek, J. F., and T. J. Schmit, 2001: Total precipitable water measurements from GOES sounder derived product imagery. *Wea. Forecasting,* **16,** 573–587.

Feltz, W. F., and J. R. Mecikalski, 2002: Monitoring high-temporal-resolution convective stability indices using the ground-based Atmospheric Emitted Radiance Interferometer (AERI) during the 3 May 1999 Oklahoma–Kansas tornado outbreak. *Wea. Forecasting,* **17,** 445–455.

——, H. B. Howell, R. O. Knuteson, H. M. Woolf, and H. E. Revercomb, 2003: Near continuous profiling of temperature, moisture, and atmospheric stability using the Atmospheric Emitted Radiance Interferometer (AERI). *J. Appl. Meteor.,* **42,** 584–597.

Hannon, S., L. L. Strow, and W. W. McMillan, 1996: Atmospheric infrared fast transmittance models: A comparison of two approaches. *Proc. Soc. Photo-Opt. Instrum. Eng.,* **2830,** 94–105.

Hawkinson, J. A., W. Feltz, and S. A. Ackerman, 2005: A comparison of GOES sounder- and cloud lidar- and radar-retrieved cloud-top heights. *J. Appl. Meteor.,* **44,** 1234–1242.

Hayden, C. M., and T. J. Schmit, 1991: The anticipated sounding capabilities of GOES-I and beyond. *Bull. Amer. Meteor. Soc.,* **72,** 1835–1846.

——, G. S. Wade, and T. J. Schmit, 1996: Derived product imagery from *GOES-8*. *J. Appl. Meteor.,* **35,** 153–162.

Hillger, D. W., and T. J. Schmit, 2007: The GOES-13 Science Test: Imager and Sounder radiance and product validations. NOAA/NESDIS Tech. Rep. 125, 75 pp.

——, ——, and J. M. Daniels, 2003: Imager and sounder radiance and product validations for the *GOES-12* Science Test.

NOAA Tech. Rep. 115, U.S. Dept. of Commerce, Washington, DC, 66 pp.

Huang, H.-L., W. L. Smith, and H. M. Woolf, 1992: Vertical resolution and accuracy of atmospheric infrared sounding spectrometers. *J. Appl. Meteor.,* **31,** 265–274.

——, and Coauthors, 2004: Minimum local emissivity variance retrieval of cloud altitude and emissivity spectrum—Simulation and initial verification. *J. Appl. Meteor.,* **43,** 795–809.

Jin, X., J. Li, C. C. Schmidt, T. J. Schmit, and J. Li, 2008: Retrieval of total column ozone from imagers onboard geostationary satellites. *IEEE Trans. Geosci. Remote Sens.,* **46,** 479–488.

Knuteson, R. O., and Coauthors, 2004a: Atmospheric Emitted Radiance Interferometer. Part I: Instrument design. *J. Atmos. Oceanic Technol.,* **21,** 1763–1776.

——, and Coauthors, 2004b: Atmospheric Emitted Radiance Interferometer. Part II: Instrument performance. *J. Atmos. Oceanic Technol.,* **21,** 1777–1789.

——, F. A. Best, D. H. DeSlover, B. J. Osborne, H. E. Revercomb, and W. L. Smith Sr., 2004c: Infrared land surface remote sensing using high spectral resolution aircraft observations. *Adv. Space Res.,* **33,** 1114–1119.

Le Marshall, J., and Coauthors, 2006a: Improving global analysis and forecasting with AIRS. *Bull. Amer. Meteor. Soc.,* **87,** 891–894.

——, J. Jung, T. Zapotocny, J. Derber, R. Treadon, S. Lord, M. Goldberg, and W. Wolf, 2006b: The application of AIRS radiances in numerical weather prediction. *Aust. Meteor. Mag.,* **55** (3), 213–217.

Leslie, L. M., J. F. Le Marshall, and W. L. Smith, 2002: Mesoscale initialisation using advanced sounder data. *Adv. Space Res.,* **30,** 2479–2484.

Li, J., J. Li, C. C. Schmidt, J. P. Nelson III, and T. J. Schmit, 2007: High temporal resolution GOES sounder single field of view ozone improvements. *Geophys. Res. Lett.,* **34,** L01804, doi:10.1029/2006GL028172.

Li, J., 1994: Temperature and water vapor weighting functions from radiative transfer equation with surface emissivity and solar reflectivity. *Adv. Atmos. Sci.,* **11,** 421–426.

——, and H.-L. Huang, 1999: Retrieval of atmospheric profiles from satellite sounder measurements by use of the discrepancy principle. *Appl. Opt.,* **38,** 916–923.

——, W. Wolf, W. P. Menzel, W. Zhang, H.-L. Huang, and T. H. Achtor, 2000: Global soundings of the atmosphere from ATOVS measurements: The algorithm and validation. *J. Appl. Meteor.,* **39,** 1248–1268.

——, C. C. Schmidt, J. P. Nelson III, T. J. Schmit, and W. P. Menzel, 2001: Estimation of total atmospheric ozone from GOES sounder radiances with high temporal resolution. *J. Atmos. Oceanic Technol.,* **18,** 157–168.

——, W. P. Menzel, F. Sun, T. J. Schmit, and J. Gurka, 2004a: AIRS subpixel cloud characterization using MODIS cloud products. *J. Appl. Meteor.,* **43,** 1083–1094.

——, ——, W. Zhang, F. Sun, T. J. Schmit, J. Gurka, and E. Weisz, 2004b: Synergistic use of MODIS and AIRS in a variational retrieval of cloud parameters. *J. Appl. Meteor.,* **43,** 1619–1634.

——, C. Y. Liu, H. L. Huang, T. J. Schmit, X. Wu, W. P. Menzel, and J. J. Gurka, 2005a: Optimal cloud-clearing for AIRS radiances using MODIS. *IEEE Trans. Geosci. Remote Sens.,* **43,** 1266–1278.

——, and Coauthors, 2005b: Retrieval of cloud microphyiscal properties from MODIS and AIRS. *J. Appl. Meteor.,* **44,** 1526–1543.

Ma, X. L., T. Schmit, and W. L. Smith, 1999: A nonlinear physical retrieval algorithm—Its application to the *GOES-8/9* sounder. *J. Appl. Meteor.,* **38,** 501–513.

Menzel, W. P., and J. F. W. Purdom, 1994: Introducing GOES-I: The first of a new generation of Geostationary Operational Environmental Satellites. *Bull. Amer. Meteor. Soc.,* **75,** 757–781.

——, F. C. Holt, T. J. Schmit, R. M. Aune, A. J. Schreiner, G. S. Wade, and D. G. Gray, 1998: Application of *GOES-8/9* soundings to weather forecasting and nowcasting. *Bull. Amer. Meteor. Soc.,* **79,** 2059–2077.

Plokhenko, Y., W. P. Menzel, G. Bayler, and T. J. Schmit, 2003: Mathematical aspects in meteorological processing of infrared spectral measurements from the GOES sounder. Part II: Analysis of spatial and temporal continuity of spectral measurements from the *GOES-8* sounder. *J. Appl. Meteor.,* **42,** 671–685.

Revercomb, H. E., and Coauthors, 2004: The path to high spectral resolution IR observing: Looking backward and forward as a new era begins with AIRS. Preprints, *20th Int. Conf. on Interactive Information and Processing Systems (IIPS) for Meteorology, Oceanography, and Hydrology,* Seattle, WA, Amer. Meteor. Soc., 14.5.

Rodgers, C. D., 1990: Characterization and error analysis of profiles retrieved from remote sounding measurements. *J. Geophys. Res.,* **95,** 5587–5595.

Schmidt, C. C., J. Li, and F. Sun, 2004: Simulation of and comparison between GIFTS, ABI, and GOES I-M Sounder ozone estimates and applications to HES. Preprints, *20th Int. Conf. on Interactive Information and Processing Systems (IIPS) for Meteorology, Oceanography, and Hydrology,* Seattle, WA, Amer. Meteor. Soc., P2.37. [Available online at http://ams.confex.com/ams/pdfpapers/71821.pdf.]

Schmit, T. J., W. F. Feltz, W. P. Menzel, J. Jung, A. P. Noel, J. N. Heil, J. P. Nelson III, and G. S. Wade, 2002: Validation and use of GOES sounder moisture information. *Wea. Forecasting,* **17,** 139–154.

——, M. M. Gunshor, W. P. Menzel, J. Li, S. Bachmeier, and J. J. Gurka, 2005: Introducing the next-generation Advanced Baseline Imager (ABI) on GOES-R. *Bull. Amer. Meteor. Soc.,* **86,** 1079–1096.

——, G. S. Wade, M. M. Gunshor, J. P. Nelson III, A. J. Schreiner, J. Li, J. Daniels, and D. W. Hillger, 2006: The GOES-N sounder data and products. Preprints, *14th Conf. on Satellite Meteorology and Oceanography,* Atlanta, GA, Amer. Meteor. Soc., P6.2. [Available online at http://ams.confex.com/ams/pdfpapers/100077.pdf.]

Schreiner, A. J., T. J. Schmit, and W. P. Menzel, 2001: Trends and observations of clouds based on GOES sounder data. *J. Geophys. Res.,* **106,** 20 349–20 363.

——, ——, G. P. Ellrod, and F. Prata, 2004: Can upper-level SO_2 be monitored using the GOES sounder? Preprints, *13th Conf. on Satellite Meteorology and Oceanography,* Norfolk, VA, Amer. Meteor. Soc., P4.7. [Available online at http://ams.confex.com/ams/pdfpapers/78300.pdf.]

Seemann, S. W., L. Jun, W. P. Menzel, and L. E. Gumley, 2003: Operational retrieval of atmospheric temperature, moisture, and ozone from MODIS infrared radiances. *J. Appl. Meteor.,* **42,** 1072–1091.

Smith, W. L., G. S. Wade, and H. M. Woolf, 1985: Combined at-

mospheric sounding/cloud imagery—A new forecasting tool. *Bull. Amer. Meteor. Soc.,* **66,** 138–141.

——, and Coauthors, 1990: GHIS—The GOES high-resolution interferometer sounder. *J. Appl. Meteor.,* **29,** 1189–1204.

——, F. W. Harrison, D. E. Hinton, H. E. Revercomb, G. E. Bingham, R. Petersen, and J. C. Dodge, 2002: GIFTS—The precursor geostationary satellite component of the future earth observing system. *Proc. IGARSS,* Toronto, ON, Canada, IEEE, 357–361.

Szyndel, M. D. E., G. Kelly, and J. N. Thépaut, 2005: Evaluation of potential benefit of assimilation of SEVIRI water vapour radiance data from Meteosat-8 into global numerical weather prediction analyses. *Atmos. Sci. Lett.,* **6** (2), 105–111.

Velden, C. S., T. L. Olander, and S. Wanzong, 1998: The impact of multispectral GOES-8 wind information on Atlantic tropical cyclone track forecasts in 1995. Part I: Dataset methodology, description, and case analysis. *Mon. Wea. Rev.,* **126,** 1202–1218.

——, S. Wanzong, I. Genkova, D. A. Santek, J. Li, E. R. Olson, and J. A. Otkin, 2007: Clear sky atmospheric motion vectors derived from the GOES sounder and simulated GOES-R hyperspectral moisture retrievals. Preprints, *Third Symp. on Future National Operational Environmental Satellites,* San Antonio, TX, Amer. Meteor. Soc., P1.28.

Wang, F., J. Li, T. J. Schmit, and S. A. Ackerman, 2007: Trade studies of hyperspectral infrared sounder on geostationary satellite. *Appl. Opt.,* **46,** 200–209.

Weisz, E., J. Li, P. Menzel, A. Heidinger, B. H. Kahn, and C.-Y. Liu, 2007: Comparison of AIRS, MODIS, *CloudSat* and *CALIPSO* cloud top height retrievals. *Geophys. Res. Lett.,* **34,** L17811, doi:10.1029/2007GL030676.

Zapotocny, T. H., W. P. Menzel, J. P. Nelson III, and J. A. Jung, 2002: Impact study of five satellite data types in the Eta Data Assimilation System in three seasons. *Wea. Forecasting,* **17,** 263–285.